Behavioral/Cognitive

Rapid Processing of Invisible Fearful Faces in the Human Amygdala

Yingying Wang,[1*] **Lu Luo,**[2*] **Guanpeng Chen,**[3,4,5] **Guoming Luan,**[6,7,8] **Xiongfei Wang,**[6] **Qian Wang,**[3,4,5] **and Fang Fang**[3,4,5]

[1]Department of Psychology and Behavioral Sciences, Zhejiang University, Hangzhou 310028, Zhejiang, China, [2]School of Psychology, Beijing Sport University, Beijing 100084, China, [3]School of Psychological and Cognitive Sciences and Beijing Key Laboratory of Behavior and Mental Health, Peking University, Beijing 100871, China, [4]IDG/McGovern Institute for Brain Research, Peking University, Beijing 100871, China, [5]Peking-Tsinghua Center for Life Sciences, Peking University, Beijing 100871, China, [6]Department of Functional Neurosurgery, Sanbo Brain Hospital, Capital Medical University, Beijing 1000932, China, [7]Beijing Key Laboratory of Epilepsy, Epilepsy Center, Sanbo Brain Hospital, Capital Medical University, Beijing 100093, China, [8]Beijing Institute for Brain Disorders, Beijing 100069, China, and [9]Department of Clinical Neuropsychology, Sanbo Brain Hospital, Capital Medical University, Beijing 100093 China

Rapid detection of a threat or its symbol (e.g., fearful face), whether visible or invisible, is critical for human survival. This function is suggested to be enabled by a subcortical pathway to the amygdala independent of the cortex. However, conclusive electrophysiological evidence in humans is scarce. Here, we explored whether the amygdala can rapidly encode invisible fearful faces. We recorded intracranial electroencephalogram (iEEG) responses in the human (both sexes) amygdala to faces with fearful, happy, and neutral emotions rendered invisible by backward masking. We found that a short-latency intracranial event-related potential (iERP) in the amygdala, beginning 88 ms poststimulus onset, was preferentially evoked by invisible fearful faces relative to invisible happy or neutral faces. The rapid iERP exhibited selectivity to the low spatial frequency (LSF) component of the fearful faces. Time-frequency iEEG analyses further identified a rapid amygdala response preferentially for LSF fearful faces at the low gamma frequency band, beginning 45 ms poststimulus onset. In contrast, these rapid responses to invisible fearful faces were absent in cortical regions, including early visual areas, the fusiform gyrus, and the parahippocampal gyrus. These findings provide direct evidence for the existence of a subcortical pathway specific for rapid fear detection in the amygdala and demonstrate that the subcortical pathway can function without con-

intracranial electroencephalogram (iEEG), which enables the direct electrophysiological recording with a high temporal resolution in the amygdala, a previous study has revealed fear-selective amygdala responses occurring at a rapid speed (Méndez-Bértolo et al., 2016). However, whether such a rapid amygdala response occurs with invisible fear is still unknown.

Based on rodent research (LeDoux, 1996), a low-road model suggests that rapid fear detection in the amygdala is enabled through a subcortical pathway, which transmits coarse information through the superior colliculus and pulvinar to the amygdala, bypassing the typically time-consuming cortical pathways (Tamietto and de Gelder, 2010). Alternatively, a multiroad model proposes that cortical pathways, which contain a multitude of shortcut anatomic routes relaying visual information to the amygdala from the extrastriate visual cortex, can be equally fast at transmitting fear as the subcortical pathway (Pessoa and Adolphs, 2010). As such, the evidence of rapid amygdala response alone cannot discriminate between the two models. To identify the contribution of the subcortical pathway, rapid amygdala response should be examined after minimizing the information transmission in cortical areas.

Unconscious fear processing offers a way to minimize information transmission and processing through cortices while retaining the subcortical contribution. The subcortical pathway is more sensitive than the cortical pathway to invisible stimuli (Tamietto and de Gelder, 2010; Diano et al., 2017). Invisible stimuli are either insufficient to evoke cortical responses or evoke much weaker responses than visible stimuli (Tamietto and de Gelder, 2010). On the contrary, invisible stimuli can evoke equal or even stronger responses in subcortical structures, including the amygdala, superior colliculus, and pulvinar, relative to visible stimuli (Morris et al., 1999; Brooks et al., 2012; Axelrod et al., 2015). Unconscious emotion processing may even adaptively increase the involvement of the subcortical pathway, as destruction of visual cortices strengthens anatomic connections of brain structures along the subcortical pathway (Tamietto et al., 2012). Furthermore, the subcortical and cortical pathways dissociate on their responses to low and high spatial frequency information. Specifically, although the cortical pathway is preferentially sensitive to the high spatial frequency information, the subcortical pathway responds to the

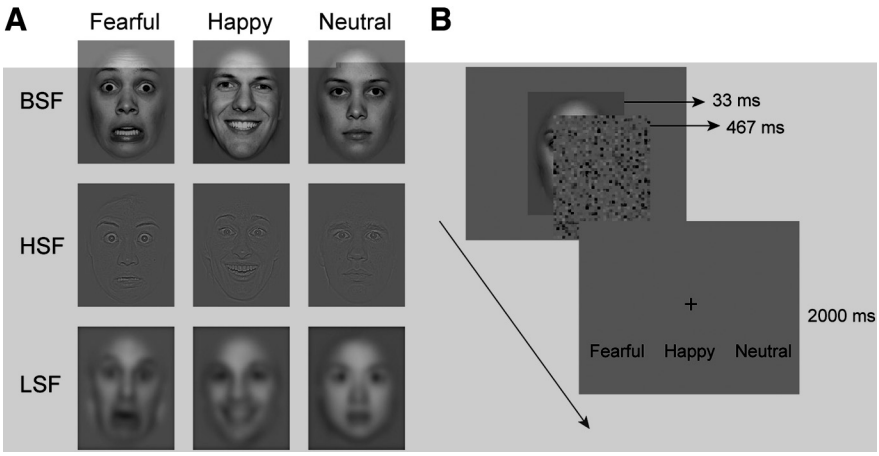

Fig re 1. Stimuli and procedure. ***A***, Examples of BSF, HSF, and LSF face images with fearful, happy, or neutral emotion. ***B***, A face image was presented for 33 ms, followed by a 467 ms white noise mask to prevent awareness of the face. Patients were instructed to identify the facial emotion and make a response within 2000 ms.

Table 2. Emo ion discrimina ion performance in each condi ion

	Accuracy (%)			*d′*		
	Fearful	Happy	Neutral	Fearful	Happy	Neutral
LSF	21.53 (13.13)	26.62 (12.00)	38.19 (22.05)	0.18 (0.33)	0.13 (0.23)	0.05 (0.12)
HSF	22.45 (11.87)	21.30 (11.87)	39.58 (25.19)	0.25 (0.31)	0.09 (0.24)	−0.00 (0.29)
BSF	38.89 (17.74)	52.08 (23.78)	44.21 (26.84)	0.70 (0.88)	1.19 (1.21)	0.86 (1.04)

Numbers in parentheses are SDs across patients.

contact was amplified using a Nicolet clinical amplifier. iEEG data at each electrode contact site were sampled at 256 Hz for one patient and 512 Hz for the remaining patients. All signals were online high-pass filtered at 0.16 Hz using a two-way least-squares finite impulse response filter and referenced to a forehead scalp electrode. Implantation sites of the EEG electrodes were determined exclusively by clinical criteria.

Stimuli

We compiled the faces of 96 different actors (48 females) posing with fearful, happy, and neutral expressions from two databases, Radboud Faces Database (https://rafd.socsci.ru.nl/RaFD2/RaFD?p=main) and NimStim Set of Facial Expressions (https://danlab.psychology.columbia.edu/content/nimstim-set-facial-expressions). Images were processed following the procedure by McFadyen et al. (2017). Specifically, all images were gray scaled, equalized in mean luminance, reshaped into the same size (5° × 6.3°), and cropped to exclude most hair and background. To create faces containing low or high spatial frequency information, the original face images (BSF) were filtered using a low-pass cutoff of <6 cycles per image (LSF) and a high-pass cutoff of >24 cycles per image (HSF), respectively. Each identity appeared in all nine conditions (3 emotions × 3 spatial frequencies). For each patient, 432 images were randomly selected from the image set, resulting in 48 images per condition. Faces with the same emotion and spatial frequency should not appear more than three times in a row. Visual stimuli were presented using MATLAB (MathWorks) software with Psychtoolbox-3 extensions (Brainard, 1997).

Experimental design

Faces were centrally displayed on an LCD screen (refresh rate, 60 Hz) for 33 ms, followed by a 467 ms white noise mask, whose mean luminance matched that of the face images (Fig. 1). A fixation cross was then presented on the screen for 2000 ms, during which patients judged whether the facial expression was fearful, happy, or neutral via key pressing. This forced-choice emotion-discrimination task was used as an objective criterion to assess emotion awareness. A chin set was used to keep the viewing distance and to keep the patient's head as still as possible. Patients were asked to avoid verbalization and minimize eye blinks. The experiment consisted of three blocks, each consisting of 144 trials and lasting ~6 min. Patients took a break after each block.

Data analysis

Patient inclusion. Of the 13 patients with amygdala electrodes, three were excluded because of excessive noise in their iEEG signal or failure to identify any discernible stimulus-evoked components during the 500 ms post-onset interval. To ensure the invisibility of masked faces, we compared each patient's performance in the forced-choice test to the one-tailed 5% cutoff (39%) of the chance distribution of correct choices (Degonda et al., 2005). One patient's performance exceeded this cutoff in emotion discrimination of LSF and HSF faces and was excluded. Despite the short presentation duration and the backward masking effect, we found that ~50% of the patients exceeded the chance distribution cutoff in emotion judgment for BSF facial expressions. So, BSF faces were not used in the iEEG experiment. Furthermore, contacts that were in the seizure onset zone or severely contaminated by epileptic activity were removed. Overall, nine patients with amygdala electrodes (10 electrodes with 33 contacts) were retained. Using the same inclusion criteria as above, six patients with EVA electrodes (8 electrodes with 28 contacts; V1, 16 contacts; V2, 8 contacts; V3, 4 contacts), four patients with FG electrodes (5 electrodes with 13 contacts), and four patients with PHG electrodes (6 electrodes with 14 contacts) were retained (Table 1).

Electrode localization. To localize the electrodes, we integrated the anatomic information of the brain provided by preoperative magnetic resonance imaging (MRI) and the position information of the electrodes provided by postoperative computer tomography (CT). For each patient, we first coregistered the postimplant CT with the preimplant anatomic T1-weighted MRI for each patient using SPM12 software (https://www.fil.ion.ucl.ac.uk/spm/software/spm12/). We then identified electrode traces in the aligned CT images and calculated the coordinates of contacts in Brainstorm (http://neuroimage.usc.edu/brainstorm; Tadel et al., 2011). To assign the anatomic label to each contact, we performed subcortical and cortical segmentations based on individual preoperative T1 MRI using FreeSurfer version 6.0 (Dale et al., 1999). We identified amygdala contacts as those localized in the amygdala and further verified them in each patient's native T1 space. An anatomic atlas for retinotopic visual areas V1–V3 (Benson et al., 2014) was used to locate EVA contacts. A high-resolution single-subject atlas (USCBrain; Joshi et al., 2022) was used to locate FG and PHG contacts. To identify cortical contacts, we projected each contact to the nearest vertex on the individual cortical surface using MATLAB function *dnsearch* and assigned the contact to a cortical area based on the projected vertex. For illustration purposes, the coordinates of contacts were normalized to the MNI space and visualized on the template brain *cvs_avg35_inMNI152*.

Preprocessing. Preprocessing was performed using the FieldTrip toolbox (Oostenveld et al., 2011) in MATLAB R2020b. Raw iEEG data from each contact were imported into MATLAB. For each contact of each electrode, epochs from −100–500 ms peristimulus onset were extracted from continuous iEEG data. Data epochs containing interictal epileptic spikes or recording artifacts were identified by visual inspection and removed from the analysis. Detrending and baseline correction (100 ms prestimulus baseline) were then performed. No filtering was applied to avoid latency artifacts because of waveform distortion. Finally, epochs were averaged across trials for each experimental condition to obtain iERPs for each contact.

iERP analysis. To determine the time points of significant iERP difference between the fearful/happy faces and the neutral faces in the LSF and HSF conditions, a cluster-based nonparametric permutation test was applied to the iERP amplitude across all contacts (Maris and Oostenveld, 2007). By clustering neighboring samples (i.e., time points) that show the

same effect, this test deals with the multiple-comparison problem while taking into account the interdependency of the data. For each sample, a paired sample *t* value was computed. All samples whose *t* value exceeded

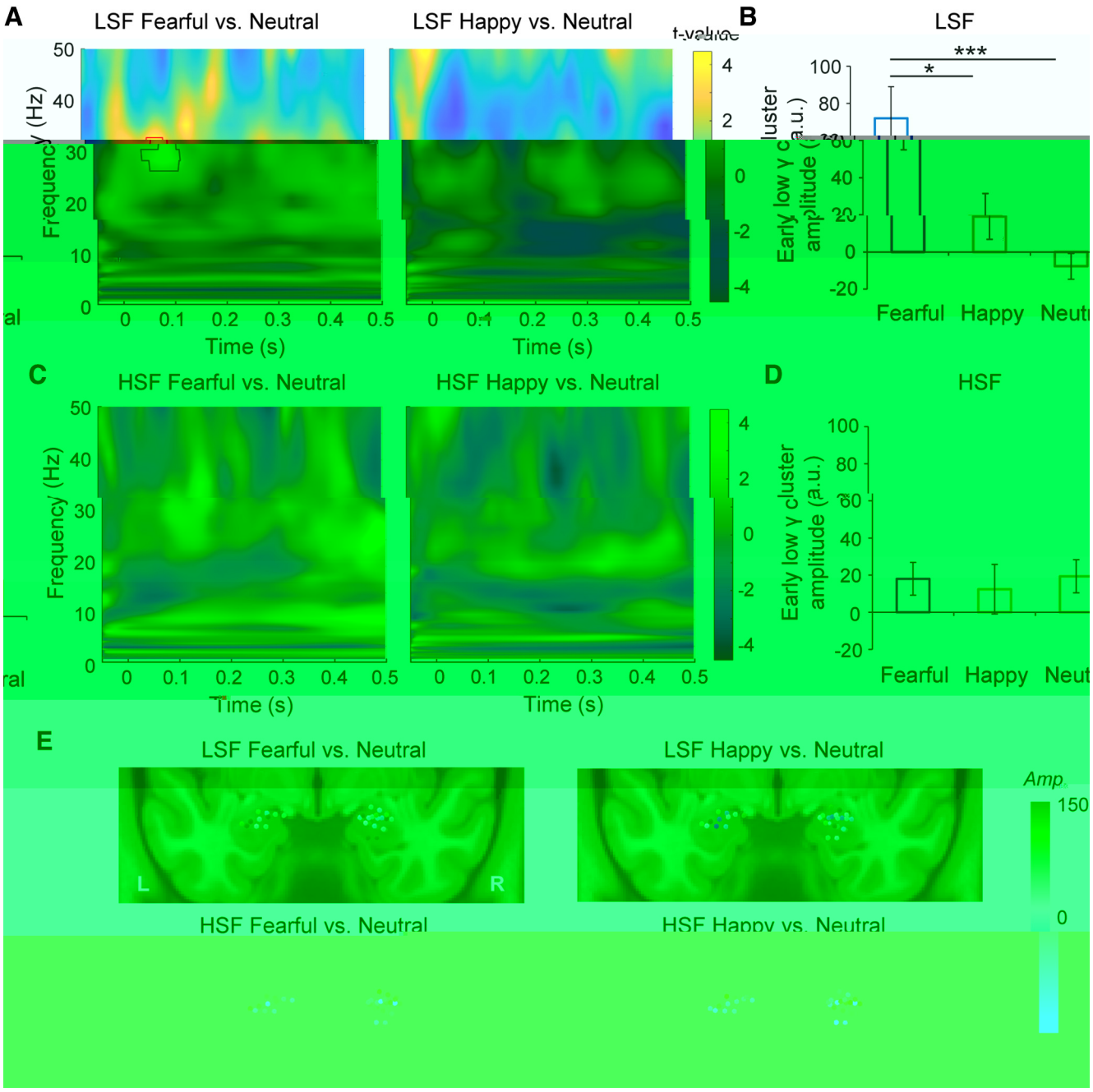

Fig re 3. Time-frequency analyses of iEEGs in the amygdala. ***A***, Statistical parametric maps of the time-frequency representation for the fearful (left) and happy (right) versus neutral face comparisons in the LSF condition. Red contour indicates the significant time-frequency cluster. ***B***, Comparison of early low gamma amplitudes (a.u., arbitrary unit; frequency, 27–33 Hz; time, 45–118 ms) between the fearful/happy and neutral faces in the LSF condition. ***C***, Statistical parametric maps of the time-frequency representation for the fearful (left) and happy (right) versus neutral face comparisons in the HSF condition. ***D***, Comparison of early low gamma amplitudes between the fearful/happy and neutral faces in the HSF condition. ***E***, The amplitude (Amp.) differences of the early low gamma cluster for single amygdala contacts. Error bars indicate SEM across contacts. ***$p < 0.001$, *$p < 0.05$ (two-tailed paired *t* tests, Bonferroni corrected).

0.01 (Fig. 2*C*, left). Meanwhile, no significant cluster was identified in the HSF condition (Fig. 2*C*, right). No response difference was observed between the happy and neutral face processing in either the LSF or HSF condition (Fig. 2*C*). We then compared the iERP responses between the LSF and HSF fearful faces. A significant cluster was identified showing a larger iERP response to the LSF than to the HSF fearful faces at an early latency (Fig. 2*D*, 50–202 ms).

To confirm the above findings, we extracted the iERP peak amplitude within the time window of 75–175 ms (Fig. 2*C*, gray shaded areas) for each emotion and SF condition. A linear mixed-effects model that included the electrodes, amygdala sides, and patients as random factors was used to examine the iERP peak amplitude difference across the emotion conditions. We found a marginally significant emotion by SF interaction effect [$\chi^2(2) = 5.51, p = 0.064$]. Consistent with the finding in the cluster-based permutation test on iERP waveforms, the main effect of emotion was significant in the LSF condition [$\chi^2(2) = 9.16, p = 0.010$] but not in the HSF condition [$\chi^2(2) = 0.63, p = 0.731$]. Specifically, the peak amplitude was larger for the LSF fearful faces than for the LSF neutral faces (Fig. 2*E*, left; $t_{(32)} = 2.84$, $p = 0.024$ Bonferroni

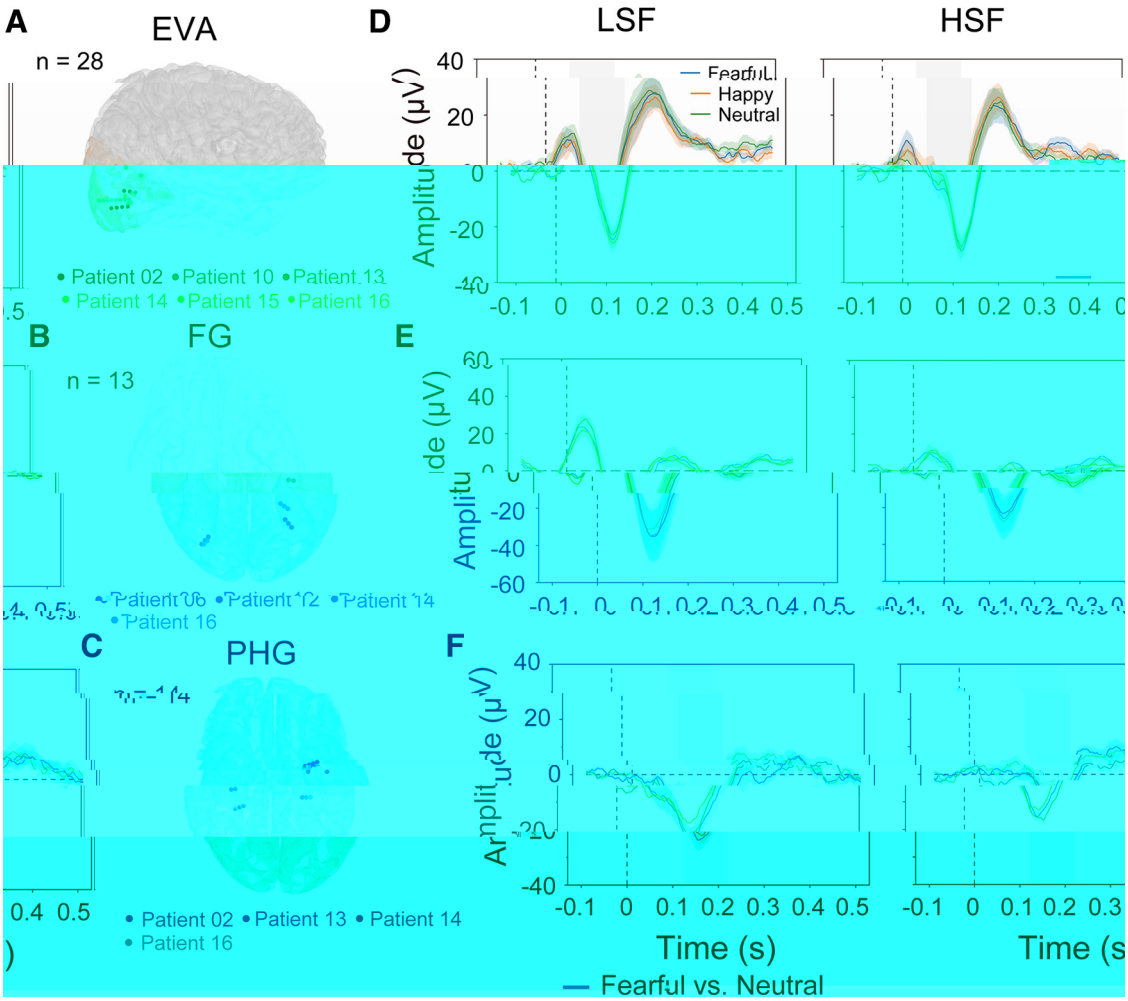

corrected, Cohen's d = 0.49). The peak amplitude difference between the LSF fearful and neutral faces was also significantly larger than that between the LSF happy and neutral faces (Fig. 2*E*, left; $t_{(32)}$ = 2.55, p = 0.048 Bonferroni corrected, Cohen's d = 0.44). No peak amplitude difference between the fearful/happy faces and the neutral faces was observed with the HSF component (p values $>$ 0.05; Fig. 2*E*, right). Altogether, these findings demonstrate a rapid, LSF-specific amygdala response to invisible fearful faces, supporting the subcortical emotion pathway model (Vuilleumier et al., 2003).

Rapid low gamma oscillations to invisible fearful faces

To further depict the frequency profiles of the iEEGs in the human amygdala, we performed a time-frequency analysis on the iEEGs in each emotion and SF condition. We found that the amygdala showed an early power increase (45–118 ms) at low gamma band (27–33 Hz) in response to the LSF fearful faces relative to the LSF neutral faces (Fig. 3*A*, left). Such a difference was not found in the LSF happy versus LSF neutral face comparison (Fig. 3*A*, right) or in the HSF condition (Fig. 3*C*). The mean amplitude of the early low gamma cluster was significantly higher for the LSF fearful faces than those for the LSF happy ($t_{(32)}$ = 2.68, p = 0.024 Bonferroni corrected, Cohen's d = 0.47) and neutral ($t_{(32)}$ = 4.50, $p < 0.001$ Bonferroni corrected, Cohen's d = 0.78) faces (Fig. 3*B*). There was no difference in the HSF condition (Fig. 3*D*; p values $>$ 0.05). We further visualized the amplitude differences of the early low gamma cluster for amygdala contacts on a brain template. As shown in Figure 3*E*, the effect was not localized to specific dominant contacts but was distributed across multiple contacts. Therefore, the rapid, LSF-specific amygdala response to the invisible fearful faces may be driven by the low gamma band oscillations.

No selective rapid response to invisible fearful faces in the visual cortex

Although the rapid LSF-specific amygdala response to the invisible fearful faces suggests a subcortical pathway for fear processing, it does not exclude the possibility that the fearful face information can be transmitted via cortical pathways. To examine this possibility, we analyzed cortical responses in patients who had electrode contacts in cortical regions along the ventral visual pathway, including the EVAs, the FG, and the PHG.

For the EVA contacts (Fig. 4*A*; 6 patients, 8 electrodes with 28 contacts in total), in contrast with the effects observed in the amygdala, we did not find any early effect in the LSF or HSF condition with the fearful/happy faces, relative to the neutral faces. A

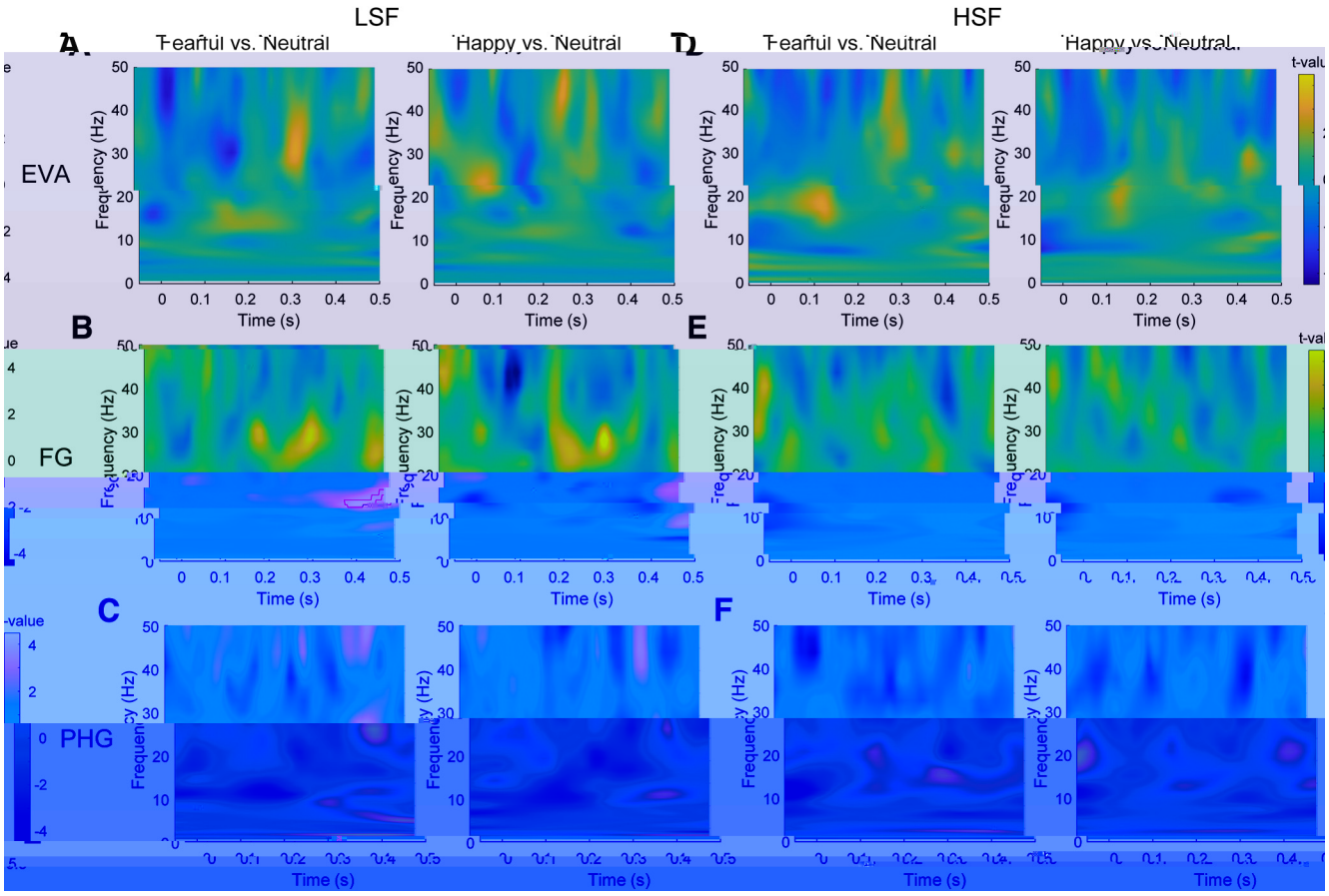

Fig re 5. Time-frequency analyses of iEEGs in visual cortex. ***A–F***, Statistical parametric maps of the time-frequency representation for the fearful/happy versus neutral face comparisons in the LSF condition in EVA (***A***), FG (***B***), and PHG (***C***) and those in the HSF condition in EVA (***D***), FG (***E***), and PHG (***F***). Red contour indicates the significant time-frequency cluster.

late-latency cluster (344–375 ms) was identified for the fearful versus neutral face comparison in the HSF condition, suggesting that the selectivity to HSF fearful faces emerged at a late stage (Fig. 4*D*, right). Next, we extracted the iERP peak amplitude within a 100 ms window surrounding the peak (i.e., 75–175 ms) for each emotion and SF condition (Fig. 4*D*, gray shaded areas). The linear mixed-effects model, same as that applied to the amygdala contacts, showed no emotion by SF interaction effect in the EVA [$\chi^2(2) = 0.05, p = 0.974$]. For the FG contacts (Fig. 4*B*; 4 patients, 5 electrodes with 13 contacts), no cluster showed significantly different iERPs to the fearful/happy versus neutral faces in either the LSF (Fig. 4*E*, left) or the HSF (Fig. 4*E*, right) condition. No emotion by SF interaction was found with the peak amplitudes [Fig. 4*E*, gray shaded areas; 75–175 ms, $\chi^2(2) = 3.69, p = 0.158$] either. For the PHG contacts (Fig. 4*C*; 4 patients, 6 electrodes with 14 contacts), no early effect was found for the fearful/happy faces relative to the neutral faces, and no emotion by SF interaction was found with the peak amplitudes [Fig. 4*F*, gray shaded areas; 125–225 ms, $\chi^2(2) = 1.17, p = 0.556$] either. Because the effects in the early visual cortex occurred much later than those in the amygdala, they could not explain the rapid response in the amygdala.

We further performed time-frequency analyses on cortical iEEGs. As shown in Figure 5, no early effects were found for the fearful/happy versus neutral face comparisons in EVA (Fig. 5*A*, *D*), FG (Fig. 5*B*,*E*), or PHG (Fig. 5*C*,*F*) in either the LSF or the HSF condition. Only late effects at the beta band were found in FG (Fig. 5*B*). Collectively, the absence of rapid responses to invisible LSF fearful faces in the ventral cortical stream argues against the possibility that the rapid discrimination of invisible fearful faces in the amygdala arises from neural activities in EVA, FG, or PHG.

Discussion

Subcortical sensory pathways have been suggested to be sufficient for rapid and unconscious processing of ecologically important stimuli, but direct electrophysiological support is lacking. Here, we reported intracranial ERP evidence that the human amygdala could selectively process invisible fearful faces containing only low spatial frequency information at an early latency of ~88 ms. Time-frequency analyses further identified that the rapid fear detection in the amygdala was associated with increased power at the low gamma frequency band. Critically, such early fear-selective responses were absent in cortical areas along the ventral visual pathway, excluding their contribution to the amygdala response. These findings strongly support the low-road model suggesting that threat information can be transmitted through a subcortical magnocellular route to the amygdala independent of the cortical pathways in humans.

Controversies remain over the response latency of the amygdala to fear. Although rapid amygdala responses to visible fearful or threatening stimuli have been reported within 100 ms after stimulus onset in magnetoencephalogram (MEG) studies (Luo et al., 2007, 2009, 2010; Bayle et al., 2009; Maratos et al., 2009; Hung et al., 2010; McFadyen et al., 2017), single-neuron and iEEG recordings in the monkey (Gothard et al.,

2007) and human (Oya et al., 2002; Krolak-Salmon et al., 2004; Mormann et al., 2008; Pourtois et al., 2010) amygdala mostly reported responses at a latency later than 100 ms. Potentially benefiting from the use of a larger sample size and more recording trials, an earlier human iEEG study found a faster amygdala response to fearful than to happy and neutral faces at 74 ms after stimulus onset (Méndez-Bértolo et al., 2016). The 88 ms effect latency to LSF fearful faces in our

Axelrod V, Bar M, Rees G (2015) Exploring the unconscious using faces. Trends Cogn Sci 19:35–45.
Bayle DJ, Henaff M-A, Krolak-Salmon P (2009) Unconsciously perceived fear in peripheral vision alerts the limbic system: a MEG study. PLoS One 4:e8207.
Benson NC, Butt OH, Brainard DH, Aguirre GK (2014) Correction of distortion in flattened representations of the cortical surface allows prediction of V1–V3 functional organization from anatomy. PLoS Comput Biol 10:e1003538.
Brainard D (1997) The Psychophysics Toolbox. Spat Vis 10:433–436.
Brooks SJ, Savov V, Allzén E, Benedict C, Fredriksson R, Schiöth HB (2012) Exposure to subliminal arousing stimuli induces robust activation in the amygdala, hippocampus, anterior cingulate, insular cortex and primary visual cortex: a systematic meta-analysis of fMRI studies. Neuroimage 59:2962–2973.
Cowey A, Stoerig P, Bannister M (1994) Retinal ganglion cells labelled from the pulvinar nucleus in macaque monkeys. Neuroscience 61:691–705.
Dale AM, Fischl B, Sereno MI (1999) Cortical surface-based analysis. Neuroimage 9:179–194.
Degonda N, Mondadori CRA, Bosshardt S, Schmidt CF, Boesiger P, Nitsch RM, Hock C, Henke K (2005) Implicit associative learning engages the hippocampus and interacts with explicit associative learning. Neuron 46:505–520.
Diano M, Celeghin A, Bagnis A, Tamietto M (2017) Amygdala response to emotional stimuli without awareness: facts and interpretations. Front Psychol 7:2029.
Fang F, He S (2005) Cortical responses to invisible objects in the human dorsal and ventral pathways. Nat Neurosci 8:1380–1385.
Garrido MI, Barnes GR, Sahani M, Dolan RJ (2012) Functional evidence for a dual route to amygdala. Curr Biol 22:129–134.
Gothard KM, Battaglia FP, Erickson CA, Spitler KM, Amaral DG (2007) Neural responses to facial expression and face identity in the monkey amygdala. J Neurophysiol 97:1671–1683.
Hung Y, Smith ML, Bayle DJ, Mills T, Cheyne D, Taylor MJ (2010) Unattended emotional faces elicit early lateralized amygdala–frontal and fusiform activations. Neuroimage 50:727–733.
Jiang Y, He S (2006) Cortical responses to invisible faces: dissociating subsystems for facial-information processing. Curr Biol 16:2023–2029.
Joshi AA, Choi S, Liu Y, Chong M, Sonkar G, Gonzalez-Martinez J, Nair D, Wisnowski JL, Haldar JP, Shattuck DW, Damasio H, Leahy RM (2022) A hybrid high-resolution anatomical MRI atlas with sub-parcellation of cortical gyri using resting fMRI. J Neurosci Methods 374:109566.
Krolak-Salmon P, Hénaff M-A, Vighetto A, Bertrand O, Mauguière F (2004) Early amygdala reaction to fear spreading in occipital, temporal, and frontal cortex: a depth electrode ERP study in human. Neuron 42:665–676.
Le QV, Nishimaru H, Matsumoto J, Takamura Y, Nguyen MN, Mao CV, Hori E, Maior RS, Tomaz C, Ono T, Nishijo H (2019) Gamma oscillations in the superior colliculus and pulvinar in response to faces support discrimination performance in monkeys. Neuropsychologia 128:87–95.
LeDoux JE (1996) The emotional brain: The mysterious underpinnings of emotional life. New York: Simon & Schuster.
Lerner Y, Singer N, Gonen T, Weintraub Y, Cohen O, Rubin N, Ungerleider LG, Hendler T (2012) Feeling without seeing? engagement of ventral, but not dorsal, amygdala during unaware exposure to emotional faces. J Cogn Neurosci 24:531–542.
Liddell BJ, Williams LM, Rathjen J, Shevrin H, Gordon E (2004) A temporal dissociation of subliminal versus supraliminal fear perception: an event-related potential study. J Cogn Neurosci 16:479–486.
Lu J, Luo L, Wang Q, Fang F, Chen N (2021) Cue-triggered activity replay in human early visual cortex. Sci China Life Sci 64:144–151.
Luo Q, Holroyd T, Jones M, Hendler T, Blair J (2007) Neural dynamics for facial threat processing as revealed by gamma band synchronization using MEG. Neuroimage 34:839–847.
Luo Q, Mitchell D, Cheng X, Mondillo K, Mccaffrey D, Holroyd T, Carver F, Coppola R, Blair J (2009) Visual awareness, emotion, and gamma band synchronization. Cereb Cortex 19:1896–1904.
Luo Q, Holroyd T, Majestic C, Cheng X, Schechter J, Blair RJ (2010) Emotional automaticity is a matter of timing. J Neurosci 30:5825–5829.
Maratos FA, Mogg K, Bradley BP, Rippon G, Senior C (2009) Coarse threat images reveal theta oscillations in the amygdala: a magneto